

Nanoscale

Accepted Manuscript



This is an *Accepted Manuscript*, which has been through the Royal Society of Chemistry peer review process and has been accepted for publication.

Accepted Manuscripts are published online shortly after acceptance, before technical editing, formatting and proof reading. Using this free service, authors can make their results available to the community, in citable form, before we publish the edited article. We will replace this *Accepted Manuscript* with the edited and formatted *Advance Article* as soon as it is available.

You can find more information about *Accepted Manuscripts* in the [Information for Authors](#).

Please note that technical editing may introduce minor changes to the text and/or graphics, which may alter content. The journal's standard [Terms & Conditions](#) and the [Ethical guidelines](#) still apply. In no event shall the Royal Society of Chemistry be held responsible for any errors or omissions in this *Accepted Manuscript* or any consequences arising from the use of any information it contains.

Improving nanoparticle diffusion in a tumor collagen matrix by photo-thermal gold nanorods

Vahid Raeesi^{1,2} and Warren Chan*¹⁻⁴

¹Department of Material Science and Engineering, University of Toronto, Toronto M5S 3E1, Canada,

²Institute of Biomaterials and Biomedical Engineering, Toronto, Ontario M5S 3G9, Canada,

³Department of Chemical Engineering Toronto, Ontario M5S 3E5, Canada,

⁴Department of Chemistry, Toronto, Ontario M5S 3H6, Canada.

Abstract. Collagen (I) impairs the targeting of nanoparticles to tumor cells by obstructing their diffusion inside dense tumor interstitial matrix. Especially, this makes large nanoparticles (> 50nm) to reside near the tumor vessels and thereby compromises their functionality. Here we propose a strategy to locally improve nanoparticle transport inside collagen (I) component of the tumor tissue. We first used heat generating gold nanorods to alter collagen (I) matrix by local temperature elevation. We then explored this impact on the transport of 50nm and 120nm inorganic nanoparticles inside collagen (I). We demonstrated increase in average diffusivity of 50nm and 120nm in the denatured collagen (I) by ~ 14 and ~ 21 fold, respectively, compared to intact untreated collagen (I) matrix. This study shows how nanoparticle-mediated hyperthermia inside tumor tissue can improve the transport of large nanoparticles (>50nm) inside a collagen (I) matrix. The ability to increase nanoparticles diffusion inside tumor stroma allows their targeting or other functionalities to take effect, thereby significant impact.

A major focus in cancer nanomedicine is to transport nanoparticles to cells within tumor milieu¹⁻³. Nanoparticles are designed as imaging probes⁴⁻⁶ and therapeutic agents⁷⁻¹⁰ to target tumor cells. To target tumor cells, nanoparticles are surface modified with a ligand that is specifically recognized by tumor cells^{11,12} and are then injected into the bloodstream. These nanoparticles are next transported through blood circulation to the tumor vessels, where it has been proposed to escape the leaky tumor vessels via enhanced permeability and retention mechanism¹³⁻¹⁵. Once nanoparticles cross the vessel wall, they need to be transported through the tumor interstitial matrix to reach the cells. Collagen (I), a major protein in the tumor interstitium¹⁶, forms a dense 3D network of fibrillar structure in the interstitial space between the tumor cells and blood vessels, and acts as the dominant physiological barrier against diffusion inside the tumor¹⁷⁻¹⁹. This poses a great challenge for many nanoparticle designs, especially for larger sizes (e.g., 100 nm) that get

Invitation for Special Issue on Cancer Nanomedicine

stuck within the collagen network²⁰. If the nanoparticles are unable to diffuse through the tumor interstitial matrix, they will reside near the vessel. There are two consequences to this: (1) targeted nanoparticles will not be able to interact with receptors on the cells, and (2) tumor retention may be shortened as they can easily diffuse out of the tumor because of high interstitial pressure (IFP)²¹. The inability of nanoparticles to transport through the tumor interstitial matrix may be a reason that a number of recent studies showed a lack of difference in total tumor accumulation between active and passive-design nanoparticles²²⁻²⁵. Hence, there is a need to develop strategies to alter the tumor matrix to enable transport of nanoparticles through it. A number of strategies have been proposed: (a) the use and incorporation of proteolytic enzyme collagenase²⁶ in the nanoparticle design²⁷⁻²⁹ and (b) design of larger nanoparticles to degrade and release smaller nanoparticles within the tumor matrix³⁰. However, these strategies have limitations. First, free collagenase can not be systematically administered as collagen is the structural protein in other organs³¹ or it may lose activity during nanoparticle formulation process³². Second, conversion of large particle assemblies to small nanoparticles require intricate design chemistry to minimize degradation during circulation³³ and rapid release³⁴ within tumor matrix before being cleared by elevated IFP³⁵. Given the heterogeneity of tumors plus variable tumor retention rates based on nanoparticle physical-chemical properties, it may be difficult to design a unified nanosystem for this purpose.

Here we proposed a strategy to locally improve nanoparticle transport inside collagen (I) component of the tumor tissue. In a collagen (I) μ -channel setup, we first introduced gold nanorods (GNRs) to alter the collagen (I) matrix under near-infrared (NIR) light stimulation. We showed local irreversible denaturation of collagen (I) fibrils by using GNR's to photo-thermally increase the local temperature to 45-55°C. We then introduced two sizes of 50nm and 120nm nanoparticles with the same surface chemistry into both treated and untreated collagen (I) μ -

Invitation for Special Issue on Cancer Nanomedicine

channels. We demonstrated increase in average diffusivity of 50nm and 120nm in the denatured collagen (I) by ~ 14 and ~ 21 fold, respectively, compared to intact untreated collagen (I) matrix. This study shows how nanoparticle-mediated hyperthermia inside tumor tissue can improve the transport of large nanoparticles ($>50\text{nm}$) inside a collagen (I) matrix.

GNRs were selected for this study because the heat generated by these nanoparticles have a theoretical photo-thermal (PTT) conversion efficiency of $> 90\%$ with NIR wavelength excitation between 700-850nm. Also, this wavelength range has been shown to yield the largest tissue penetration depth³⁶. GNRs have been applied for single cancer therapy as a hyperthermia agent³⁷⁻⁴⁰ or as part of a combinatorial strategy for synergistic killing⁴¹⁻⁴³ of tumor cells. The experimental set-up to study the effect of GNRs generated heat on transport through a collagen (I) matrix is described in figures 1a and b. The glass μ -chip had two reservoirs, which were connected through a μ -channel. We filled the channel with bovine collagen (I) solution and neutralized it to form rigid gel structure in 4hrs. The collagen (I) matrix appeared turbid inside the μ -channel (Figure 1c). Reflectance confocal imaging revealed a porous structure with randomly oriented collagen fibers at a concentration ranging from 2-7 mg/mL (Figure S1). A 7mg/ml collagen concentration (Figure 1d) was used for most experiments as it was in the range of the reported collagen (I) contents in tumors⁴⁴. The transport mode in our setup was diffusion (derived by concentration gradient) as there was no convective flow (Peclet number ~ 0). GNRs were synthesized via a directional growth of gold seeds in cetyltrimethyl ammonium bromide (CTAB) surfactant and ascorbic acid^{41,45} (See Materials Methods in the Supplement Section). Next, GNRs were coated with polyethylene glycol (PEG) to stabilize them in a buffer medium. The GNRs had an average length to width ratio of 28nm x 7nm (Figure 2a), longitudinal absorption peak at 750nm and a transverse peak at 520nm (Figure 2b). 30 μ l GNRs were added to one reservoir and the other reservoir was filled with equal volume of phosphate buffered saline (PBS). Then we used a

Invitation for Special Issue on Cancer Nanomedicine

continuous wavelength near-IR laser (785nm) to excite the GNRs and the temperature was monitored using thermal imaging. We first correlated the relationship between GNR concentration and laser power to control temperature elevation (Figure 2c and S2). We utilized this characterization to study the effect of heat on collagen (I) gel structure in the μ -channels. We raster irradiated the channel horizontally with a 5 mm diameter laser beam in one side of the μ -channel. We optimized the GNR concentration (6nM), laser power density ($3\text{W}/\text{cm}^2$) so that the channel exposed-area exhibit an average temperature between 45-55°C, in the range of reported collagen (I) denaturation temperatures^{46,47} (See figure 2d) When the μ -channel was heated, the exposed area became clear (Figure 2d). The heated medium converted from a dense hydrogel to a liquid-like medium. We detected no reflectance signal from collagen fibrils within a photo-thermally exposed area (Figure 2e and f) with 88% loss of turbidity (as measured by absorbance measurements at 405 nm⁴⁸) compared to non-exposed areas (Figure 2g), suggesting the disappearance of collagen fibers. After cooling, the fiber structure did not re-form, indicating irreversible denaturation of collagen fibers. This is likely due to the transformation of the native triple helical structure into a random coiled structure as reported by previous studies^{49,50}. This change in conformation was further confirmed by the observation of agglomerates at the bottom of the channel wall (Figure 2h).

The GNR's PTT experiments clearly showed that the fibrillar structure was altered in the collagen (I) matrix. We next evaluated whether this change in collagen (I) matrix will lead to an increase in transport of spherical nanoparticles. We selected gold nanoparticles of 50 and 120 nm core diameters as model particle systems. These spherical gold nanoparticles were synthesized using a hydroquinone-seed mediated growth method and surface coated with polyethylene glycol and AlexaFluor dye molecules using previous developed methods from our laboratory (Figure 3a, See materials and methods). This dye was selected because it can be excited at 647 nm and the

Invitation for Special Issue on Cancer Nanomedicine

emission is far from the plasmon band of the gold nanoparticles, so that minimal quenching of the dye by gold nanoparticle surface would occur. The 50nm and 120nm nanoparticles showed plasmon peaks at 535nm and 595nm, respectively (Figure 3b). TEM images revealed their size and shape with narrow size distribution (Figure S3) and this was supported by dynamic light scattering measurements with a PDI < 0.06.

To demonstrate GNR's PTT effect on diffusion, we added GNRs (6nM) in one reservoir of both μ -channels and then illuminated the channel with a laser for 6min using our previously optimized conditions. We then added the fluorescently-tagged nanoparticles on top of the GNRs reservoir and then traced the motion of the nanoparticles as it was diffusing along the collagen (I) matrix channel length using confocal fluorescence microscopy (Materials and Methods). Images were recorded in 12hrs at different distances along the μ -channel and processed using ImageJ and Matlab to develop spatio-temporal intensity profiles and calculate diffusivity values, respectively. The confocal fluorescent images in figure 3c illustrate the diffusion of the 50nm (red) and 120nm (green) nanoparticles along the collagen (I) matrix channel before and after PTT treatment. The red/green colors are meant to distinguish between 50nm and 120nm nanoparticles and not indicative of actual emission channel. The diffusion direction is from left (high concentration) to right (low concentration) at the same time point and the position for each particle size. Regardless of nanoparticle size, in untreated collagen (I) matrix, the average intensity along the channel length is low and most of the nanoparticles are populated at the left end of the channel whereas in a photo-thermally treated (PTT) collagen (I) matrix, we detected higher average fluorescence intensity through the entire length of the channel. Qualitatively, we can make two conclusions. (1) At a defined time t , the number of nanoparticles along the length of the channel is higher in PTT-treated channel for both nanoparticle sizes. (2) At the same nanoparticle concentration, the penetration depth through the collagen (I) matrix is increased when PTT is applied. This suggested

Invitation for Special Issue on Cancer Nanomedicine

that there was an increase in the diffusivity of nanoparticles through the collagen (I) matrix after PTT. We further scrutinized these results by developing intensity profile along the mid-channel for each particle size. Figure 3d,e show temporal intensity profiles for the 50nm nanoparticles in control and PTT-treated μ -channels, respectively. The PTT process increased the rate of intensity change compared to an intact collagen (I) matrix, regardless of the penetration depth. For a fixed penetration depth (same concentration gradient), the rate of increase in intensity can be a measure of how resistant the medium is against diffusion. For penetration depth of 0-500 μ m, we calculated ~ 9 fold increase in the intensity rate for PTT treated channel. This means in PTT denatured collagen (I) matrix, 50nm nanoparticles reached their initial local maximum concentration 9 times faster than intact collagen (I) matrix (control). We then plotted the normalized intensity versus penetration depth at $t = 4$ hrs which was the required time for $x = 0$ (Reference point) to reach its maximum point (Figure 3f). For penetration depth of 100 μ m-1000 μ m, we found 2.1-18.0 fold increase in the intensity. We inferred in PTT treated channel, the local concentration of 50nm nanoparticles at different penetration depth was increased. Also, an increase in the intensity from 0% to 54% at $x = 1,000\mu$ m suggests that the penetration depth in PTT-treated channel was increased. The effect of the PTT process for 120 nm particles followed the same trend as 50 nm nanoparticles, shown in Figure 3g, h. 120nm nanoparticles reached saturation in PTT-treated channel in ~ 3 hrs while in untreated channel the signal for the same spot started to saturate after 12 hrs. 120 nm nanoparticles showed fluorescent signals at 500 μ m for PTT treat collagen (I) matrix as compared to untreated matrix. This suggested more than a 300 μ m increase in penetration depth for 120nm nanoparticles. We quantified the change in collagen (I) matrix diffusivity (D) by developing intensity profiles versus penetration distance at fixed time points and fitted the data to fick's law solution:

Invitation for Special Issue on Cancer Nanomedicine

$$C(x, t) = A \operatorname{erfc}\left(\frac{x}{2\sqrt{Dt}}\right) \quad (1)$$

where C denotes nanoparticle intensity, x represents diffusion distance and t shows imaging time. Figure 4 demonstrates the change in diffusivity of 50 nm and 120 nm inside the collagen (I) matrix during the PTT. In the absence of PTT, 50nm nanoparticles showed an effective diffusivity value of $1.62 \times 10^{-8} \text{ cm}^2/\text{s}$ through the collagen (I) matrix channel compared to $3.39 \times 10^{-9} \text{ cm}^2/\text{s}$ for the 120nm sized gold nanoparticles. Interestingly, PTT process increased the effective diffusivity of the 50 nm gold nanoparticle by ~ 14 fold ($2.36 \times 10^{-7} \text{ cm}^2/\text{s}$) versus ~ 21 ($7.22 \times 10^{-8} \text{ cm}^2/\text{s}$) fold for 120 nm nanoparticles. From this data, the diffusivity of the 120 nm nanoparticle is 4.5 times slower than the 50 nm through the collagen (I) matrix. Considering inverse proportionality of D vs. hydrodynamic radius in the Stokes-Einstein equation, a 2.4 times decrease in diffusivity based on core nanoparticle diameters is calculated. This discrepancy may be explained by a combination of different hydrodynamic radius after PEGylation/Dye conjugation and surface charge density between the 50nm and 120nm nanoparticles. Interestingly, we found PTT process showed ~ 1.5 fold higher effect on diffusivity enhancement for 120nm versus 50nm. If one rules out average measurement errors and that PTT from GNRs homogeneously denatures collagen matrix, one would expect the same ratio of enhancement in diffusivity for both nanoparticle sizes. However, from Stokes-Einstein equation, D is inversely proportional to the term μR , where μ is medium viscosity and R is hydrodynamic radius. This suggests that the PTT effect from GNRs may inhomogeneously denature collagen fibers inside its network. This is supported by our earlier data that random coiled microstructures were detected at the bottom of the channel, suggesting that inhomogeneous viscosity appears inside the denatured collagen (I) matrix. So, what does this mean in terms of nanotherapeutic delivery to tumor cells? Larger nanoparticles such as the 120 nm can carry more therapeutic agents to cancer cells than smaller nanoparticles but previous studies showed that these larger nanoparticles typically reside near the tumor vasculature. There

Invitation for Special Issue on Cancer Nanomedicine

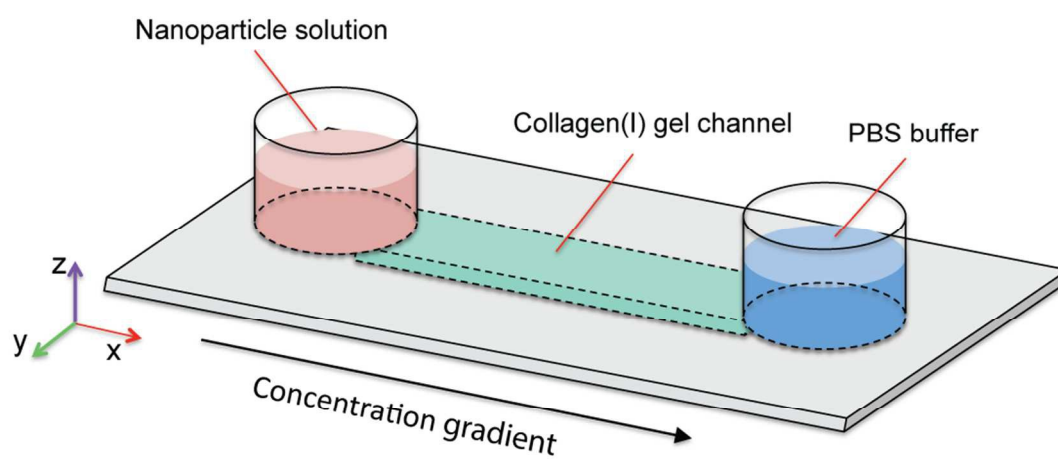
could be a trade-off between the diffusivity of smaller nanoparticles through the tumor extracellular matrix versus the larger nanoparticles. Here, we showed the transport limitations of a larger nanoparticle can be negated by thermally denaturing the collagen (I) matrix first, which can potentially remove the barrier for transport of larger nanoparticles to tumor cells.

In conclusion, we used an in vitro model to show that a 2-step process can enhance the penetration of nanoparticles transport within a collagen matrix. The first step requires the denaturation of collagen structure by using gold nanorods heating, which effectively opens up the collagen (I) matrix for larger nanoparticles to transport through. We clearly showed a deeper penetration depth of 50 and 120 nm spherical gold nanoparticles within the collagen (I) matrix after gold nanorod priming. Further experiments will require the confirmation of improved transport of larger nanoparticles through the tumor matrix in animal models. The tumor extracellular matrix may prevent the transport of nanoparticles to the targeted tumor cells and the use of gold nanorods heating may prime the tumor for the “actual” nanoparticle therapeutic or diagnostic formulation to be successfully delivered to the tumor cells. This may be the case for both direction injection of “second” nanoparticles into tumors as well as via a systemic inject, where nanoparticles may have to diffuse through the matrix to reach the targeting cells. The gold nanorods may be introduced into the tumor via direct or system injection. In vivo, even if these nanoparticles do not penetrate deeply, the ability to heat and denature the localized tumor matrix may allow more nanoparticles to diffuse through. The incorporation of heat-generating components that denatures the tumor extracellular matrix may allow entire nanosystems to be transported through the tumor extracellular matrix and achieve specific tumor cell targeting.

Invitation for Special Issue on Cancer Nanomedicine

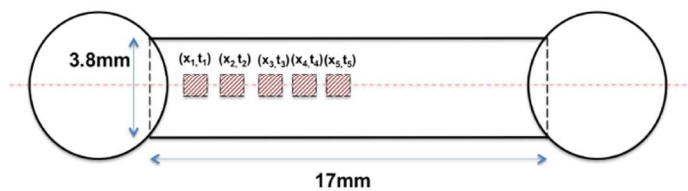
Acknowledgements. WCWC would also like to acknowledge the Canadian Institute of Health Research, Natural Sciences and Engineering Research Council, Prostate Cancer Canada for supporting his research program

A.



B.

Channel volume: 30ul
Channel height(h): 0.4mm



C.



D.

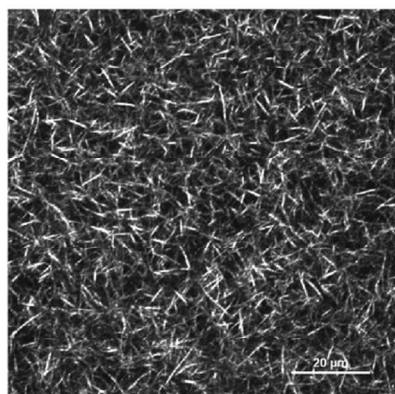
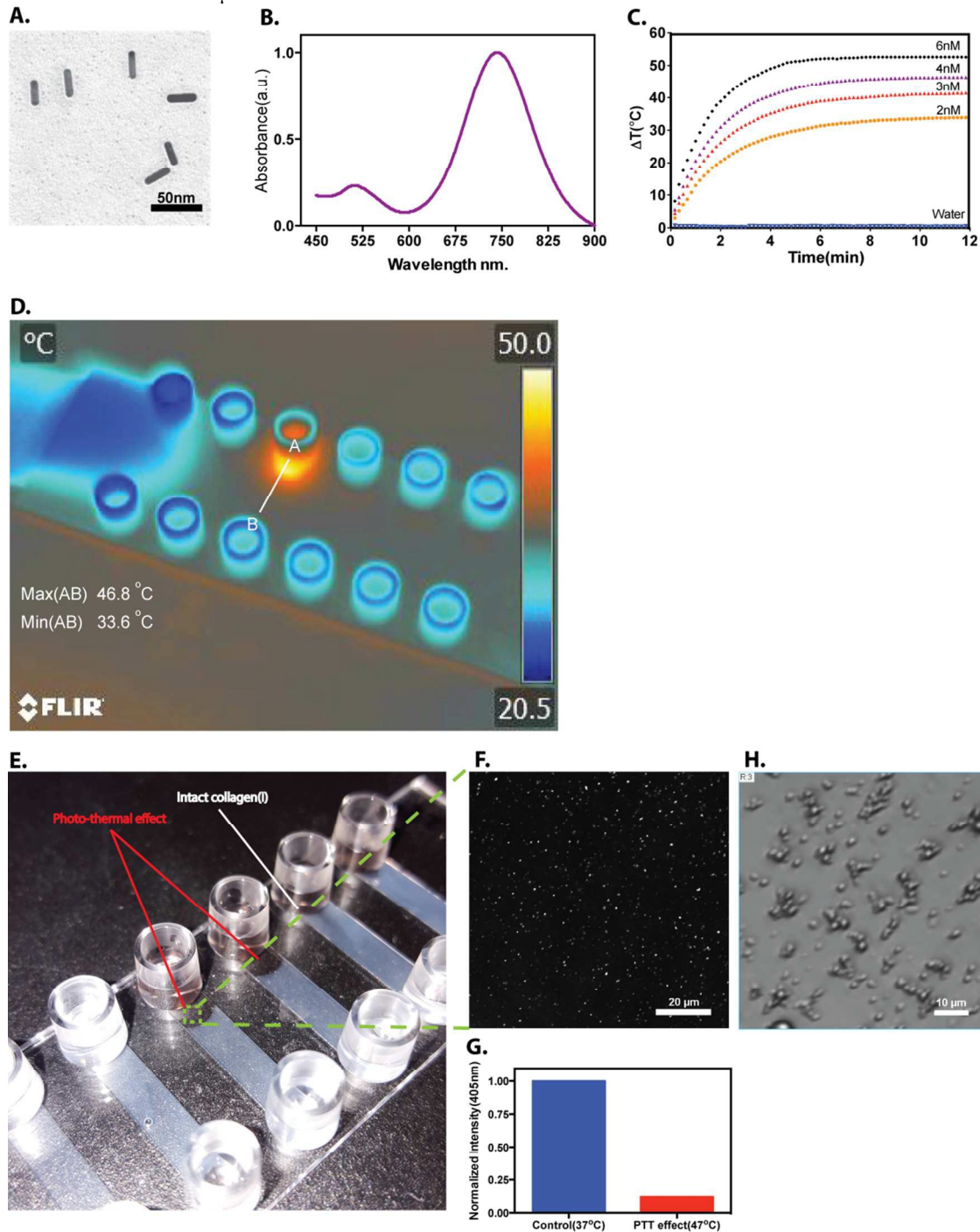


Figure 1 | Design of the tumor collagen (I) matrix barrier model. **A)** Schematic of the μ -chip design. **B)** XY- plane projection of the μ -channel: The μ -channel dimensions are 17mm x 3.8mm x 0.4mm (L x W x H), which can accommodate 30 μ l collagen (I) hydrogel. The thin glass slide at the bottom would enable imaging by confocal fluorescence microscopy along the μ -channel. **C)** Optical image of the μ -channels filled with intact collagen (I) proteins between the reservoirs appear turbid. **D)** Reflectance confocal image of the collagen (I) matrix at 7mg/ml concentration inside a μ -channel.



Invitation for Special Issue on Cancer Nanomedicine

Figure 2| Effect of photo-thermal GNRs on collagen (I) matrix. **A)** Representative TEM image of gold nanorods with an aspect ratio of ~ 4 . **B)** Absorption spectrum of gold nanorods, which showed longitudinal and transverse plasmon peaks at 750nm and 520nm, respectively. **C)** Photo-thermal characteristics of GNRs under fixed 3W/cm² laser power density as a function of concentration. **D)** Thermographic image of the μ -chip during PTT process on GNRs injected into the channel. The GNR elevated the local channel temperature (red/yellow color) to an average of $\sim 47^\circ\text{C}$ after raster illumination of laser beam (3W/cm²) over $\sim 8\text{mm}$ channel length for 6 min. **E)** Optical image of the collagen μ -channels after PTT process. The collagen hydrogel appeared clear. **F)** Reflectance confocal image of the channel after PTT. **G)** Normalized absorption of collagen (I) hydrogel at 405nm before and after PTT process. **H)** Transmittance confocal image of the PTT affected channel area.

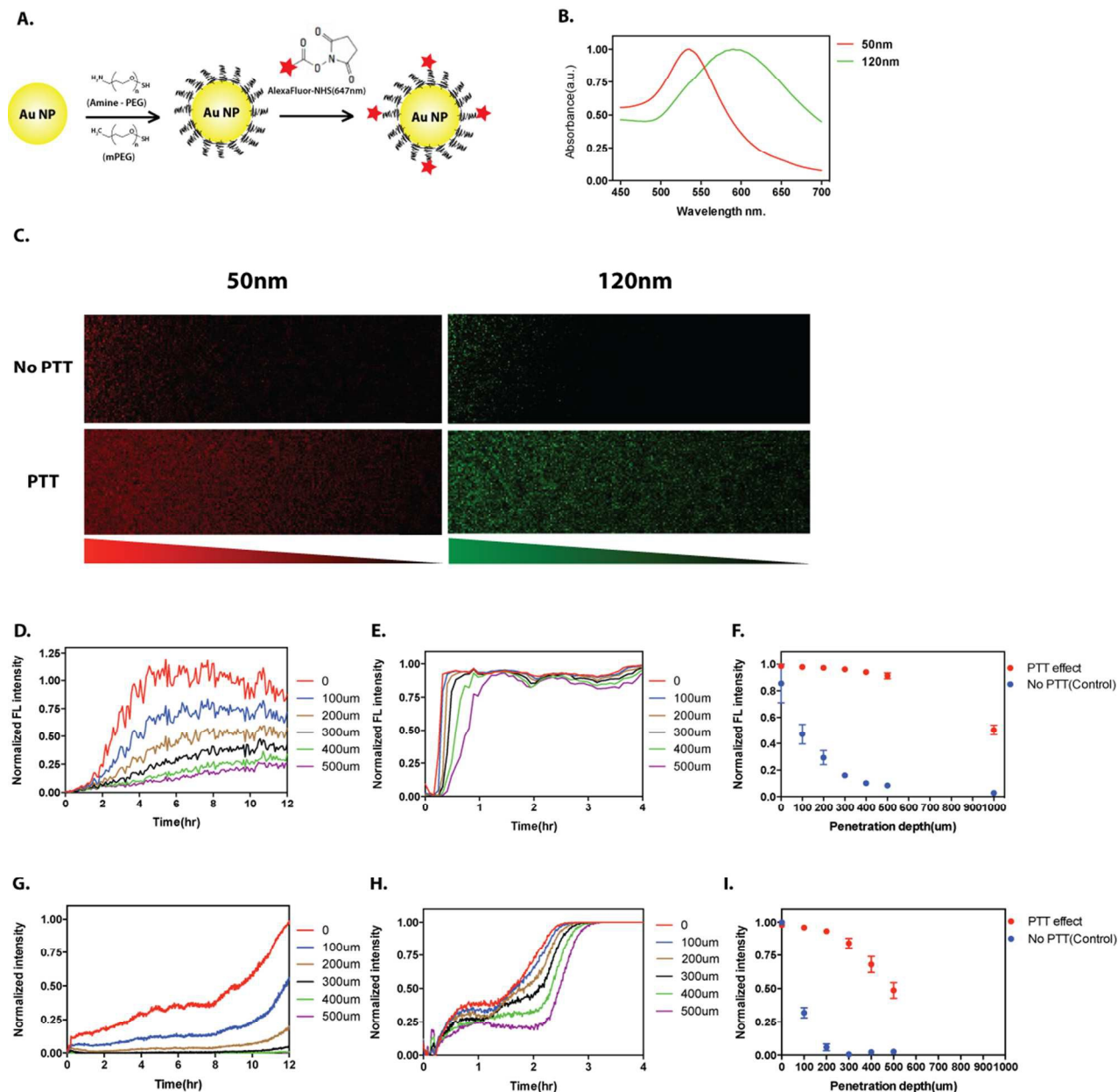


Figure 3| Effect of Photo-thermal GNRs on diffusion inside collagen (I). **A)** Schematic of the process to PEGylate and surface modify the gold nanoparticles with AlexFluor647nm. **B)** Absorption spectrum of fluorescent Alexafluor (647nm)-conjugated gold nanoparticles. **C)** Representative confocal images of two parallel channels with and without PTT process and 50nm and 120nm fluorescently tagged gold nanoparticles. The red/green colors are meant to

Invitation for Special Issue on Cancer Nanomedicine

distinguish between 50nm and 120nm nanoparticles and not indicative of actual emission channel. **D)** Mid-channel intensity profile for 50nm without PTT. **E)** Mid-channel intensity profile for 50nm with PTT. **F)** Penetration depth profile for 50nm at $t=4$ hrs with and without PTT. **G)** Mid-channel intensity profile for 120nm without PTT. **H)** Mid-channel intensity profile for 120nm with PTT. **I)** Penetration depth profile for 120nm at $t=2.5$ hrs with and without PTT.

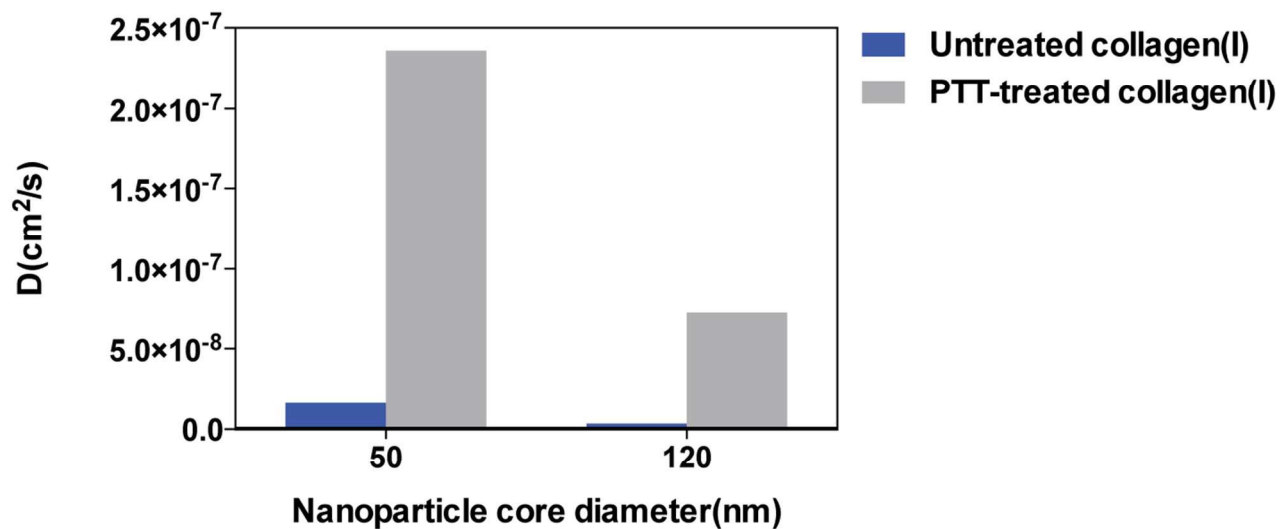


Figure 4| Effect of GNRs PTT on the diffusivity of 50nm and 120nm gold nanoparticles inside collagen (I).

References:

- 1 R. K. Jain and T. Stylianopoulos, *Nat Rev Clin Oncol*, 2010, **7**, 653–664.
- 2 E. Ruoslahti, S. N. Bhatia and M. J. Sailor, *The Journal of Cell Biology*, 2010, **188**, 759–768.
- 3 W. Jiang, B. Y. Kim, J. T. Rutka and W. C. Chan, *Expert Opin. Drug Deliv.*, 2007, **4**, 621–633.
- 4 J. V. Jokerst, T. Lobovkina, R. N. Zare and S. S. Gambhir, *Nanomedicine*, 2011, **6**, 715–728.
- 5 V. P. Zharov and D. O. Lapotko, *IEEE J. Select. Topics Quantum Electron.*, **11**, 733–751.
- 6 L. Y. T. Chou and W. C. W. Chan, *Advanced Healthcare Materials*, 2012, **1**, 714–721.
- 7 L. Zhang, F. Gu, J. Chan, A. Wang, R. Langer and O. Farokhzad, *Clin Pharmacol Ther*, 2007, **83**, 761–769.
- 8 J. Hrkach, D. Von Hoff, M. M. Ali, E. Andrianova, J. Auer, T. Campbell, D. De Witt, M. Figa, M. Figueiredo, A. Horhota, S. Low, K. McDonnell, E. Peeke, B. Retnarajan, A. Sabnis, E. Schnipper, J. J. Song, Y. H. Song, J. Summa, D. Tompsett, G. Troiano, T. Van Geen Hoven, J. Wright, P. LoRusso, P. W. Kantoff, N. H. Bander, C. Sweeney, O. C. Farokhzad, R. Langer and S. Zale, *Science Translational Medicine*, 2012, **4**, 128ra39–128ra39.
- 9 C. J. Langer, *Proc. Am. Soc. Clin. Oncol.*, 2005, **96**.
- 10 D. Yoo, H. Jeong, C. Preihs, J.-S. Choi, T.-H. Shin, J. L. Sessler and J. Cheon, *Angew. Chem. Int. Ed.*, 2012, n/a–n/a.
- 11 A. P. R. Johnston, M. M. J. Kamphuis, G. K. Such, A. M. Scott, E. C. Nice, J. K. Heath and F. Caruso, *ACS Nano*, 2012, **6**, 6667–6674.
- 12 T. A. ElBayoumi and V. P. Torchilin, *Clinical Cancer Research*, 2009, **15**, 1973–1980.
- 13 M. E. Davis, Z. G. Chen and D. M. Shin, *Nat Rev Drug Discov*, 2008, **7**, 771–782.
- 14 C. J. Cheng, G. T. Tietjen, J. K. Saucier-Sawyer and W. M. Saltzman, *Nat Rev Drug Discov*, 2015.
- 15 S. D. Perrault, C. Walkey, T. Jennings, H. C. Fischer and W. C. W. Chan, *Nano Lett.*, 2009, **9**, 1909–1915.
- 16 Y.-L. Yang, S. Motte and L. J. Kaufman, *Biomaterials*, 2010, **31**, 5678–5688.
- 17 P. A. Netti, D. A. Berk, M. A. Swartz, A. J. Grodzinsky and R. K. Jain, *Cancer Research*, 2000, **60**, 2497–2503.
- 18 2012, 1–11.
- 19 O. Tredan, C. M. Galmarini, K. Patel and I. F. Tannock, *JNCI Journal of the National Cancer Institute*, 2007, **99**, 1441–1454.
- 20 A. Pluen, Y. Boucher, S. Ramanujan, T. D. McKee, T. Gohongi, E. di Tomaso, E. B. Brown, Y. Izumi, R. B. Campbell, D. A. Berk and R. K. Jain, *Proceedings of the National Academy of Sciences*, 2001, **98**, 4628–4633.
- 21 L. T. Baxter and R. K. Jain, *Microvascular research*, 1989.
- 22 E. A. Sykes, J. Chen, G. Zheng and W. C. W. Chan, *ACS Nano*, 2014, **8**, 5696–5706.
- 23 E. Huynh and G. Zheng, *WIREs Nanomed Nanobiotechnol*, 2013, **5**, 250–265.
- 24 S. Kunjachan, R. Pola, F. Gremse, B. Theek, J. Ehling, D. Moeckel, B. Hermanns-Sachweh, M. Pechar, K. Ulbrich, W. E. Hennink, G. Storm, W. Lederle, F. Kiessling and T. Lammers, *Nano Lett.*, 2014, **14**, 972–981.
- 25 D. B. Kirpotin, *Cancer Research*, 2006, **66**, 6732–6740.

Invitation for Special Issue on Cancer Nanomedicine

- 26 M. Magzoub, S. Jin and A. S. Verkman, *The FASEB Journal*, 2007, **22**, 276–284.
- 27 T. T. Goodman, P. L. Olive and S. H. Pun, *International journal of ...*, 2007.
- 28 S. Murty, T. Gilliland, P. Qiao, T. Tabtieng, E. Higbee, A. A. Zaki, E. Puré and A. Tsourkas, *Part. Part. Syst. Charact.*, 2014, **31**, 1307–1312.
- 29 S. J. Kuhn, S. K. Finch, D. E. Hallahan and T. D. Giorgio, *Nano Lett.*, 2006, **6**, 306–312.
- 30 C. Wong, T. Stylianopoulos, J. Cui, J. Martin, V. P. Chauhan, W. Jiang, Z. Popovic, R. K. Jain, M. G. Bawendi and D. Fukumura, *Proceedings of the National Academy of Sciences*, 2011, **108**, 2426–2431.
- 31 R. K. Jain, *J. Clin. Oncol.*, 2013, **31**, 2205–2218.
- 32 M. R. Villegas, A. Baeza and M. Vallet Regí, *ACS Appl. Mater. Interfaces*, 2015, 151013114646000.
- 33 F. Tewes, E. Munnier, B. Antoon, L. Ngaboni Okassa, S. Cohen-Jonathan, H. Marchais, L. Douziech-Eyrolles, M. Soucé, P. Dubois and I. Chourpa, *European Journal of Pharmaceutics and Biopharmaceutics*, 2007, **66**, 488–492.
- 34 A. P. Esser-Kahn, S. A. Odom, N. R. Sottos, S. R. White and J. S. Moore, *Macromolecules*, 2011, **44**, 5539–5553.
- 35 R. K. J. S R Chary, *Proceedings of the National Academy of Sciences of the United States of America*, 1989, **86**, 5385–5.
- 36 Z. Qin and J. C. Bischof, *Chem. Soc. Rev.*, 2012, **41**, 1191.
- 37 C. Ungureanu, R. Kroes, W. Petersen, T. A. M. Groothuis, F. Ungureanu, H. Janssen, F. W. B. van Leeuwen, R. P. H. Kooyman, S. Manohar and T. G. van Leeuwen, *Nano Lett.*, 2011, **11**, 1887–1894.
- 38 T. B. Huff, M. N. Hansen, Y. Zhao, J.-X. Cheng and A. Wei, *Langmuir*, 2007, **23**, 1596–1599.
- 39 W.-S. Kuo, C.-N. Chang, Y.-T. Chang, M.-H. Yang, Y.-H. Chien, S.-J. Chen and C.-S. Yeh, *Angew. Chem. Int. Ed.*, 2010, NA–NA.
- 40 T. B. Huff, L. Tong, Y. Zhao, M. N. Hansen, J.-X. Cheng and A. Wei, *Nanomedicine*, 2007, **2**, 125–132.
- 41 T. S. Hauck, T. L. Jennings, T. Yatsenko, J. C. Kumaradas and W. C. W. Chan, *Adv. Mater.*, 2008, **20**, 3832–3838.
- 42 K. C. Hribar, M. H. Lee, D. Lee and J. A. Burdick, *ACS Nano*, 2011, **5**, 2948–2956.
- 43 D. Wang, Z. Xu, H. Yu, X. Chen, B. Feng, Z. Cui, Bin Lin, Q. Yin, Z. Zhang, C. Chen, J. Wang, W. Zhang and Y. Li, *Biomaterials*, 2014, **35**, 8374–8384.
- 44 S. Ramanujan, A. Pluen, T. D. McKee, E. B. Brown, Y. Boucher and R. K. Jain, *Biophysical Journal*, 2002, **83**, 1650–1660.
- 45 N. R. Jana, *Small*, 2005, **1**, 875–882.
- 46 C. A. Miles and A. J. Bailey, *Proceedings of the Indian Academy of Sciences - Chemical Sciences*, **111**, 71–80.
- 47 L. Bozec and M. Odlyha, *Biophysical Journal*, 2011, **101**, 228–236.
- 48 A. O. Brightman, B. P. Rajwa, J. E. Sturgis, M. E. McCallister, J. P. Robinson and S. L. Voytik-Harbin, *Biopolymers*, 2000, **54**, 222–234.
- 49 N. T. Wright and J. D. Humphrey, *Annu. Rev. Biomed. Eng.*, 2002, **4**, 109–128.
- 50 2013, 1–10.
- 51 S. D. Perrault and W. C. W. Chan, *J. Am. Chem. Soc.*, 2009, **131**, 17042–17043.

Invitation for Special Issue on Cancer Nanomedicine

Nanoscale Accepted Manuscript